© 2007 OSA/CQO 2007

Adjunct Spectral Entanglement in Entanglement Swapping and Type-I Fusion

Travis S. Humble and Warren P. Grice
Computing and Computational Sciences Directorate
Oak Ridge National Laboratory, Bldg. 5600, MS-6016, Oak Ridge, TN
humblets@ornl.gov, gricew@ornl.gov

Abstract: We show how adjunct spectral entanglement affects polarization-based entanglement swapping and type-I fusion gates and we explain why the concurrences of the subsequently entangled states are distinctively dependent on the initial joint spectral amplitudes.
©2007 Optical Society of America.
OCIS codes: (270.0270) Quantum Optics; (200.0202) Optical Computing

The relative ease with which polarization-entangled photons are generated using spontaneous parametric down-conversion (SPDC) enables realizations of the two-qubit gates underlying many proposals of quantum computation. But adjunct photonic degrees of freedom can affect this entanglement, e.g., correlated frequencies arising from energy conservation yield spectral entanglement that distinguishes between polarizations. We report on how spectral entanglement affects the performance of two polarization-based two-qubit gates: (1) entanglement swapping [1], which enables offline state preparation in the quantum circuit model [2], and (2) type-I fusion [3], proposed for preparing cluster states in the approach of one-way quantum computing [4].

We consider identical type-II SPDC sources to produce polarization-entangled photon pairs (1,2) and (3,4), where the state of (1,2)

$$\left|\psi_{12}\right\rangle = \frac{1}{\sqrt{2}}\int d\omega \int d\omega' \left[f_{12}(\omega,\omega')\left|h_1(\omega),v_2(\omega')\right\rangle + g_{12}(\omega,\omega')\left|v_1(\omega),h_2(\omega')\right\rangle\right] \tag{1}$$

is described by the joint spectra $f_{12}(\omega,\omega')$ and $g_{12}(\omega,\omega')$ and a similar expression holds for pair (3,4). In type-II SPDC, the spectral differences correlate with polarization and the joint spectra satisfy $f_{12}(\omega,\omega')=g_{12}(\omega',\omega)$. In general, the joint spectrum is inseparable with respect to frequency and may be well approximated by [5]

$$f_{12}(\omega,\omega') = (\pi\sigma\sigma'\sqrt{1-\mu^2})^{-1/2}\exp\left[-\left(\Delta\omega^2/\sigma^2 - 2\mu\Delta\omega\Delta\omega'/\sigma\sigma' + \Delta\omega'^2/\sigma'^2\right)\Big/2(1-\mu^2)\right]. \tag{2}$$

The difference frequencies $\Delta\omega=\omega-\omega_0$ and $\Delta\omega'=\omega'-\omega_0$ are defined relative to half the pump-pulse frequency ω_0 while the linear correlation μ and the marginal bandwidths σ and σ' are given in terms of experimental parameters in [5]. The relevant source configurations are shown in panels (a) $f_{12}(\omega,\omega')=f_{34}(\omega,\omega')$ and (b) $f_{12}(\omega,\omega')=f_{34}(\omega',\omega)$ of Fig. 1.

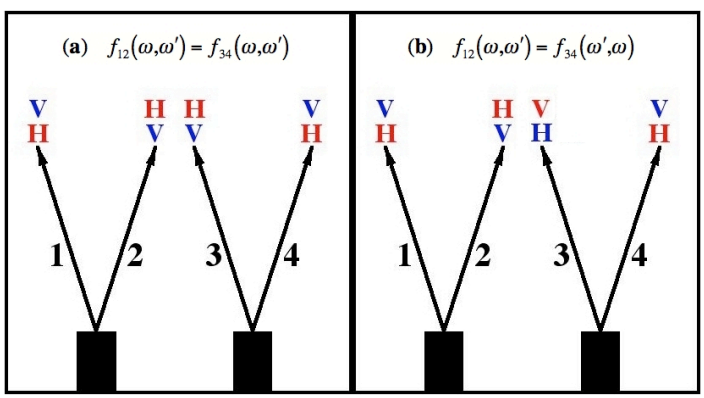

Fig. 1. Two configurations for a pair of type-II SPDC sources that supply the input to entanglement swapping and type-I fusion gates. In (a) similarly polarized photons in modes 2 and 3 have identical marginal spectra, in (b) oppositely polarized photons in modes 2 and 3 have identical spectra. Boxes (blue) and circles (red) denote the spectral properties of the photons while H and V denote polarization. The black boxes denote the entanglement sources and any additional linear optical elements.

Entanglement swapping is implemented by sending photons 2 and 3 to a 50:50 beam splitter whose output is discriminated with respect to polarization before detection. Certain coincidences between detectors correspond to preparation of photons (1,4) in the frequency-reduced, polarization-entangled state

$$\rho_{14} = \left(\left|h_1,v_4\right\rangle\left\langle h_1,v_4\right| + G_{14}\left|h_1,v_4\right\rangle\left\langle v_1,h_4\right| + G_{14}^*\left|v_1,h_4\right\rangle\left\langle h_1,v_4\right| + \left|v_1,h_4\right\rangle\left\langle v_1,h_4\right|\right)\Big/2, \tag{4}$$

where

$$G_{14} = \int d\omega \int d\omega' \int d\omega'' \int d\omega''' f_{12}(\omega,\omega'')g_{34}(\omega'',\omega')^* g_{12}(\omega,\omega''')f_{34}(\omega''',\omega'). \tag{5}$$

The concurrence of ρ_{14} is $C_{14}=|G_{14}|$. For source configuration (a), this evaluates to

$$C_{14}^{(a)} = 2\sigma\sigma'\sqrt{1-\mu^2}\Big/\left(\sigma^2+\sigma'^2\right) \tag{6}$$

© 2007 OSA/CQO 2007

while for configuration (b) the concurrence following entanglement swapping is

$$C_{14}^{(b)} = 4\sigma^2\sigma'^2\left(1-\mu^2\right)\Big/\left[\left(\sigma^2+\sigma'^2\right)\sqrt{\left(\sigma^2+\sigma'^2\right)-4\mu^2\sigma^2\sigma'^2}\right]. \tag{7}$$

In type-I fusion, photons 2 and 3 enter a polarizing beam splitter after which photons in one of the exit ports are rotated by π/4 and discriminated with respect to polarization before being detected. For a single-photon detection event the polarization state of the remaining three-particle system is unitarily equivalent to

$$\rho_{134} = \frac{1}{2}\left(\left|h_1,v_3,h_4\right\rangle\left\langle h_1,v_3,h_4\right| + G_{134}\left|h_1,v_3,h_4\right\rangle\left\langle v_1,h_3,v_4\right| + G_{134}^*\left|v_1,h_3,v_4\right\rangle\left\langle h_1,v_3,h_4\right| + \left|v_1,h_3,v_4\right\rangle\left\langle v_1,h_3,v_4\right|\right) \tag{8}$$

where

$$G_{134} = \int d\omega \int d\omega' \int d\omega'' \int d\omega''' f_{12}(\omega,\omega'')g_{34}(\omega''',\omega')^* g_{12}(\omega,\omega''')f_{34}(\omega'',\omega')^*. \tag{9}$$

The tripartite concurrence $C_{1(34)} = |G_{134}|$ is derived from the residual tangle, and for source configurations (a) and (b), respectively, evaluates to

$$C_{134}^{(a)} = C_{14}^{(b)} \qquad \text{and} \qquad C_{134}^{(b)} = C_{14}^{(a)}. \tag{10}$$

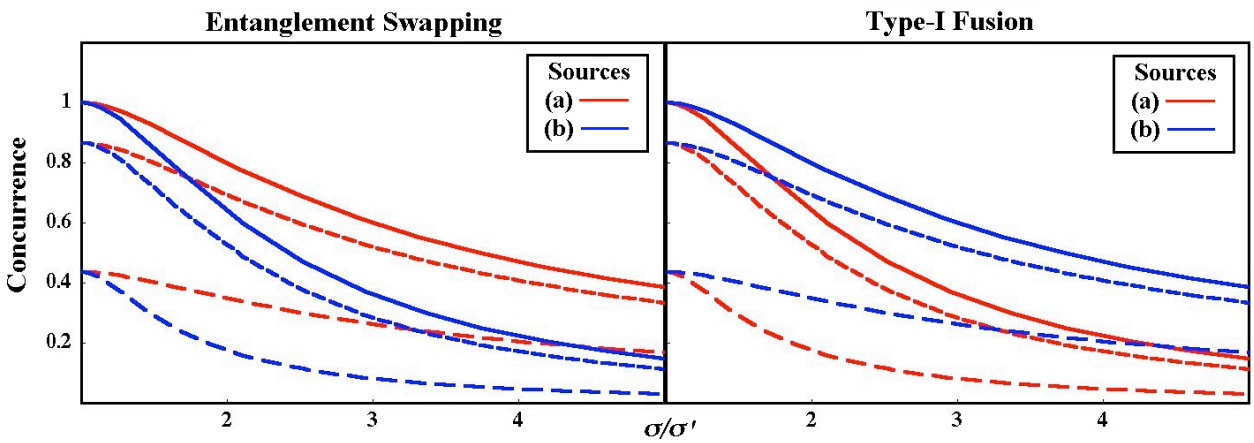

Fig. 2. The bipartite and tripartite concurrences resulting from entanglement swapping and type-I fusion, respectively. In the left panel, the bipartite concurrence obtained with source configurations (a) and (b) of Fig 1 are plotted as a function of σ/σ′ for various values of the linear correlation μ: 0 (solid lines), -0.5 (short-dashed lines), -0.9 (long-dashed lines). In the right panel, similar results are shown for the tripartite concurrence obtained with source configurations (a) and (b) and the same values of the linear correlation. Note that Eq. (10) relates the curves in the two panels.

Entanglement swapping and type-I fusion differ in terms of which source configuration optimizes the resulting concurrence. For entanglement swapping, source configuration (a) leads to a larger concurrence than source configuration (b), while the converse statement is true for type-I fusion. The basis for the latter distinction lies in the different detection strategies of the two protocols. In entanglement swapping, the Bell-state measurement performs best when there is an absence of which-path information in the photons leaving the beam splitter. For entanglement swapping, if the oppositely polarized photons with different spectra in Fig. 1(a) meet at a beam splitter, then monitoring the color as well as the polarization of the outputted photons will not distinguish between the two interference processes, i.e., h_3 transmitted and v_2 reflected versus h_2 reflected and v_3 transmitted. In contrast, if the oppositely polarized photons having identical spectra in Fig. 1(b) meet at the beam splitter, then by monitoring the frequency of the detected photons one can discern the source of each photon.

In the case of type-I fusion, the parity-check measurement erases the polarization information pertaining to the incident photon before detection. The erasure step works best with the source configuration in (b), where oppositely polarized photons are spectrally identical. This is because subsequently monitoring the color as well as the polarization of the detected photon does not permit one to distinguish between whether two vertical or two horizontal photons met at the polarizing beam splitter. If instead the oppositely polarized photons with different spectra from source (b) were to pass through the polarizing beam splitter, then the input into the polarization rotator in the monitored output mode could be determined based on the color of the detected photon. This spectral distinguishability would in turn discriminate between the two interference processes and compromise the quantum eraser. Finally, neither the bipartite nor the tripartite concurrence is maximal using either source configuration because of the cross correlations between spectral and polarization degrees of freedom carried by photons 1 and 4.

References

1. J.-W. Pan, D. Bouwmeester, H. Weinfurter, and A. Zeilinger, "Experimental entanglement swapping: Entangling particles that never interacted," Phys. Rev. Lett. **80**, 3891 (1998).
2. E. Knill, R. Laflamme, and G. J. Milburn, "A scheme for efficient quantum computation with quantum optics," Nature **409**, 46 (2001).
3. D. E. Browne and T. Rudolph, "Resource-efficient linear optical quantum computation," Phys. Rev. Lett. **95**, 010501 (2005).
4. R. Raussendorf and H. J. Briegel, "A one-way quantum computer," Phys. Rev. Lett. **86**, 5188 (2001).
5. T. S. Humble and W. P. Grice, "Spectral effects in quantum teleportation," Phys. Rev. A **75**, 022307 (2007).